Journal of Atmospheric and Solar-Terrestrial Physics 71 (2009) 1807–1813

Contents lists available at ScienceDirect

Journal of Atmospheric and Solar-Terrestrial Physics

journal homepage: www.elsevier.com/locate/jastp

Calibrated measurements of PMSE strengths at three different locations observed with SKiYMET radars and narrow beam VHF radars

N. Swarnalingam [a,*], W.K. Hocking [a], W. Singer [b], R. Latteck [b]

[a] Department of Physics and Astronomy, University of Western Ontario, London, Ontario, Canada
[b] Leibniz Institute of Atmospheric Physics, Kühlungsborn, Germany

ARTICLE INFO

Article history:
Received 7 December 2008
Received in revised form
12 June 2009
Accepted 18 June 2009
Available online 1 July 2009

PACS:
3394
3332
3334
3311
3394
6974
3360

Keywords:
PMSE
Radar calibration
Polar mesosphere

ABSTRACT

While PMSE are a well recognized summer phenomenon in the polar regions, debate still exists on their relative strengths as function of latitude and longitude. Different radar design and noise calibration procedures complicate comparison between sites. Here, we use radars at multiple sites, some with a common design, to better determine the radar backscatter cross-section, and hence compare PMSE strengths. Five radars at Yellowknife (62.5°N, 114.3°W), Andenes (69.3°N, 16.0°E) and Resolute Bay (75.0°N, 95.0°W) in the northern hemisphere were used to observe PMSE during July 2005. At Yellowknife, data were collected for thirteen days. In other two locations data were collected continuously for the full month of July. The radars were independently calibrated using the same method, and absolute backscatter cross-sections were determined. Resolute Bay is close to both the magnetic and geomagnetic north poles, and inside the auroral oval, while the other two sites are under the auroral oval on some occasions. Inter-comparison of the calibrated observations indicates that the strength of the PMSE at Yellowknife and Andenes are comparable, and both are significantly stronger than at Resolute Bay.

1. Introduction

Polar Mesosphere Summer Echoes (PMSE) are strong coherent radar echoes from the cold summer mesosphere at high latitudes. Following their unexpected discovery in the late seventies by Ecklund and Balsley (1981) several active radar campaigns were conducted in the American and European sectors of the northern hemisphere (e.g., Czechowsky and Rüster, 1985; Hoppe et al., 1988; Röttger et al., 1988). Results of these campaigns led to a debate among researchers, since the well known classical coherent radar backscatter theories such as neutral turbulent backscatter theory and Fresnel (partial) reflection theory had failed to explain the observed features of PMSE (see Cho and Kelley, 1993; Rapp and Lübken, 2004 and references therein). After an intense three decades of theoretical and experimental studies, it is now widely accepted that the cold mesopause temperature ($T<150$ K) and nanometer size charged ice particles play a decisive role in producing PMSE. Nevertheless, understanding the physical process that causes the small scale fluctuations that are necessary to produce radar echoes, remains a challenging task.

2. Uncertainties in geographic and geomagnetic relative strengths

The relative strengths of PMSE at different radar sites, and hence latitudinal and longitudinal variations, still remains an open question. Since the inclusion of dynamical processes in thermal models predicts much colder mesopause temperature near the poles than at mid-latitudes (e.g., Garcia and Solomon, 1985), it is not unreasonable to expect more intense and frequent occurrences of PMSE towards the poles. Recently, Rapp and Lübken (2004) argued that the temperature dependence agrees with experiments at least in regard to occurrence rates, especially in the European sector of the northern hemisphere. On the other hand, Huaman et al. (2001) reported a low occurrence rate of PMSE at Resolute Bay (75.0°N, 95.0°W) observed by a 51.5 MHz VHF radar. The Resolute Bay VHF radar has been continuously monitoring PMSE since 1997. The low occurrence rates of PMSE at this site have recently raised many important questions on the appropriateness of current PMSE theories, as well as on the

* Corresponding author.
E-mail address: nswarna2@uwo.ca (N. Swarnalingam).

1364-6826/$ - see front matter
doi:10.1016/j.jastp.2009.06.014

capabilities of the Resolute Bay radar itself. Following this, recently this radar system was carefully calibrated using cosmic noise variations with the additional help of a commercially available calibrated noise source (Swarnalingam and Hocking, 2006, 2007). The calibrated PMSE echoes at this site indicate that PMSE strength at this location is indeed weak compared with the strength observed at other high latitude radar sites (Swarnalingam, 2007; Swarnalingam et al., 2009).

Knowing the geographic distribution of PMSE in terms of calibrated signal strengths is vital to understand these echoes. Over the years, many PMSE experiments have been conducted in the northern hemisphere region. However, most of the observed results were not in the form of absolute calibrated signal strengths. Although a few experimental results are available in the form of calibrated signal strengths for selected case studies, these results were not obtained using a common standard method of radar calibration and signal processing (e.g., Kelley and Ulwick, 1988; Hoppe et al., 1988; Röttger and La Hoz, 1990; Inhester et al., 1990; Hocking and Röttger, 1997; Röttger, 2001). Furthermore, these experiments were not conducted during the same time interval. Instead, the data were collected on an ad hoc basis over a long period of time. Studies in the southern hemisphere have also been conducted but are limited in number, since they started only a decade or so ago (e.g., Woodman et al., 1999; Jarvis et al., 2005; Morris et al., 2007).

In order to understand the geographical distribution and hence the latitudinal and longitudinal dependence of PMSE, there is a need to monitor them with commonly designed radars that share a standard method of absolute calibration and signal processing. The importance of this concept was proposed by Woodman (2003) as a resolution at the Tenth International Workshop on Technical and Scientific Aspects of MST Radar held in Peru in May 2003. Following this, radars from the SKiYMET meteor radar network were used for the first time for such a study during the boreal summer of 2005.

The SKiYMET radar network consists of a number of near identical radars spread across large geographical regions in the northern and southern hemispheres. As the first stage of this study, radars located at Yellowknife in Canada (62.5°N, 114.3°W) and Andenes in Norway (69.3°N, 16.0°E) were used to observe PMSE. In addition to these, a design employing a four-antenna Quartet-Mode radar at Resolute Bay (75.0°N, 95.0°W) was also involved in this study. In this paper, we present the results of thirteen days of SKiYMET observation at Yellowknife (in the interval of 1–21 July 2005), four days of SKiYMET observation at Andenes (in the interval of 1–21 July 2005) and nine days of the Quartet-Mode radar observation at Resolute Bay (in the interval of 11–21 July 2005). The experiments were run for periods of 2–6 hours on a daily basis, covering both day and night. The results are compared with PMSE observations from two traditional MST radars (the Resolute Bay VHF radar and the ALWIN radar) located at Resolute Bay and Andenes, respectively. Data for these two traditional radars were collected continuously in the interval 1–31 July 2005. We consider that these experiments with the SKiYMET radars at Yellowknife and Andenes will be a prelude to more extensive experiments using other existing SKiYMET (and similar) systems.

3. Experiment setup and noise calibration

The SKiYMET radar is an all-sky interferometric meteor radar originally intended to observe winds in the mesosphere region using radio scatter from meteor trails. In general, the SKiYMET radar uses a single 3-element crossed Yagi antenna for transmission and five independent 2-element crossed Yagi antennas for reception. At Yellowknife, the system operates at 35.65 MHz with a 6 kW transmitter peak power, and at Andenes it operates at 32.55 MHz with a 12 kW transmitter peak power. Both radars have a vertical resolution of 2 km. In order to use SKiYMET radars to study PMSE, they were electronically modified to operate like traditional coherent radars, by coherently adding the signals on all five receivers after compensating for phase delays in each channel. As a result, the receiver polar diagram has nine grating lobes, each with a moderate width of 5° half-power-half-width (HPHW). One lobe points vertically, four point 30° off-vertical and another four point 42° off-vertical. Fig. 1 shows the receiver polar diagram of the Yellowknife SKiYMET radar system (upper panel). It is plotted in $\sin(\theta)\cdot\sin(\phi)$ coordinates, where θ and ϕ refer to the off-vertical and azimuthal angles, respectively. The lower panel of the figure shows the projection of the nine grating lobes (HPFW) of this radar into the sky (at 14:00 ST). While the white dot in the center refers the geographic north pole, the white dash–dash line shows the path of the centroid of this radar in a sidereal day.

No traditional SKiYMET radar is located at Resolute Bay, but instead we used a so-called Quartet-Mode radar, comprising four 2-element Yagi antennas at the corners of square with sides of length $\lambda/2$. This is embedded within the existing Main-Mode radar antenna array. The Quartet-Mode radar uses a wider beam (35° HPHW) for both transmission and reception in the vertical direction (monostatic mode).

The recent calibration work at Resolute Bay by Swarnalingam and Hocking (2006) involved comparing the diurnal variation of cosmic noise power (also called sky noise) against the recorded

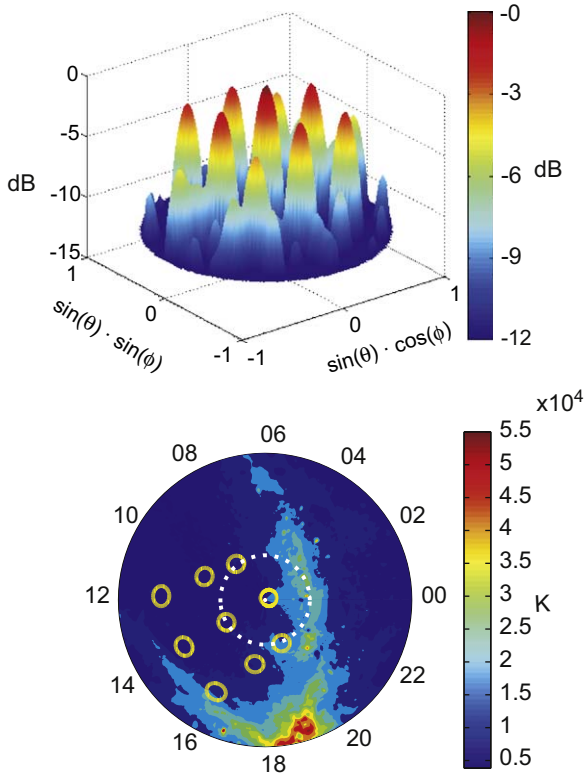

Fig. 1. Upper panel shows a 3D view of the reception polar diagrams plotted for the SKiYMET radar system located at Yellowknife. The lower panel shows the sky noise temperature for the northern hemisphere at 35.65 MHz (the operational frequency of the Yellowknife SKiYMET radar). The sky noise temperature is plotted in right ascension—declination coordinates with the geographic north pole at the center (white dot). The yellow circles show projections of the nine grating lobes (HPFW) of the Yellowknife SKiYMET radar into the sky. The white dash–dash line shows the path of the centroid of this radar in a sidereal day.

radar power (in arbitrary digital units), and then developing a conversion constant between these two powers. Since the pathways to the radar receiver for both the backscattered signal and the cosmic noise are the same, the same conversion constant can be used to estimate the absolute signal strength of the backscattered power. The advantage of this calibration method is that it can be directly applied to any MST radar anywhere in the world as long as the cosmic noise variation above the site is known. Detailed discussions of this method can be found in Swarnalingam and Hocking (2007) and Swarnalingam et al. (2009). However, for completeness we briefly describe the method here. (Following the calibration work at Resolute Bay, the method was also used by Kirkwood et al. (2007) to compare PMSE strengths at Kiruna (68°N) and Wasa (73°S), Antarctica.)

In order to calibrate all other radars which were involved in this study we applied the same method at each location independently. In a radar system, the total noise power that reaches the radar receiver (P_{Rx}) and the true sky noise power detected by the antenna array (P_{Sky}), for times when the transmitter is turned off, can be linked through a linear relationship as follows:

$$P_{Rx} = e^R\{P_{Sky} + N_{Loc}\} + (1 - e^R)N_{Lin} \quad (1)$$

where e^R is the system efficiency for reception. The quantity N_{Loc} refers to the local noise power that originates in the surrounding area, mainly due to human activities. While the diurnal variation of P_{Sky} depends on local sidereal time, N_{Loc} remains approximately constant. N_{Lin} refers to the transmission line noise. The noise power P_{Rx} is thus fed into the receiver, and consequently recorded in the computer in arbitrary digital units. However, an additional constant noise power N_{Rx} is also detected directly by the receiver due to various pieces of equipment inside the receiver building and also due to internal noise within the receiver itself. The relationship between the input received by the receiver and the recorded power (P_{Rec}) can be written as

$$P_{Rec} = \frac{G_S}{N \cdot M \cdot L}\{P_{Rx} + N_{Rx}\} \quad (2)$$

where G_S is the conversion factor between Watts and digital units. N and M represent the actual number of coherent integrations and number of bits used in the pulse-coding, respectively. These quantities appear in Eq. (2) as a result of coherent averaging (Swarnalingam, 2007; Swarnalingam et al., 2009).

L was introduced to handle the situation in which complementary codes are used. In such situations confusion may arise with the actual value of M. In complementary codes, each code will contain a pair of elements such that the second element is the complement of the first element (Schmidt et al., 1979). Therefore, the actual number of pulses are two times M. In order to generalize the above equation to be valid regardless of the chosen pulse-coding, the parameter L is introduced. It corresponds to the number of elements of codes. It will take a value 2 if complementary codes were used, otherwise it stays as 1.

Combining Eqs. (1) and (2) will lead to the final calibration equation:

$$P_{Rec} = \frac{G_S^*}{N \cdot M \cdot L}\left\{P_{Sky} + N_{Loc} + \left(\frac{1 - e^R}{e^R}\right)N_{Lin} + N_{Rx}\right\} \quad (3)$$

where $G_S^* = (G_S \cdot e^R)$. By comparing the variation of P_{Rec} against P_{Sky}, and applying a linear regression fit, we can determine G_S^*.

The cosmic power variation above the radar site can be calculated from sky survey maps available close to the radar operational frequency. Currently two main sky surveys close to our radar operational frequencies are available. The first one at 30 MHz was published by Cane (1978) and the other at 22 MHz was published by Roger et al. (1999). Although both surveys cover more than 90% of the northern hemisphere, we have decided to use the second one since it has better angular resolution. The map's sky noise temperature values were transferred to radar frequency equivalent temperatures by assuming that the cosmic radiation decreases with frequency by a power law of mean spectral index $\beta = 2.50$. The actual value of β has been a subject of debate in the literature, but it is now widely accepted that its value is very close to 2.50, especially for the VHF range (e.g., Bridle, 1967; Sironi, 1974; Webster, 1974; Haslam et al., 1981). Nevertheless, in order to get the most accurate value for β we have performed our own analysis and comparison, especially in the northern mid and high latitude region, by comparing five surveys within the frequency range 22–178 MHz (Swarnalingam, 2007). The five surveys that were used in our analysis were at 22 MHz by Roger et al. (1999), 30 MHz by Cane (1978), 45 MHz by Campistron et al. (2002), 85 MHz by Landecker and Wielebinski (1970) and 178 MHz by Turtle and Baldwin (1962). Based on this comparison, it was found that the Roger et al. (1999) 22 MHz survey maintains a β value of 2.50 with respect to the other surveys. The error is only 1% if the 30 MHz survey is excluded, otherwise the possible error is about 5%. Therefore, in our calibration work it was decided to use $\beta = 2.50$. Furthermore, our estimated value for β is in good agreement with the β used by Campistron et al. (2002) and Roger et al. (1999).

A two dimensional convolution between the radar polar diagram and the equivalent sky noise temperature was then carefully applied, in order to calculate the sky noise temperature diurnal variations. However, possible ionospheric absorption has to be considered in the estimation of G_S^*. For the SKiYMET and ALWIN radars this was taken into account by comparing the experiment days with the nearest riometer data (available at: http://www.dcs.lancs.ac.uk/iono/cgi-bin/riometers). We compared each sidereal day of sky noise collected by the radar with the baseline curve for the geographically closest riometer at the frequency closest to our own. From this comparison, we were able to identify the absorption signatures, which are typically on a relatively short time scale compared with the quiet day curve. The sky noise collected by radar during these time intervals were eliminated in our calibration procedure. Elimination of short time interval of data would not affect our final calibration results, since our procedure uses many sidereal days of sky noise data (see Swarnalingam et al., 2009, Figs. 2 and 3). For the Resolute Bay radar, we used quiet day noise variations that were identified from a large data set collected by radar (the Resolute Bay radar has been continuously operated both in summer and winter seasons starting from 1997). For the calibration work presented here, twelve days of data were selected in the interval of 26–30 June, 1–7 July, 23–27 July and 26–30 August from the data collected during the 2005 boreal summer.

4. Calculation of PMSE backscatter cross-sections

For all five radars, the received PMSE peak power P_R in Watts was estimated using the corresponding G_S (or G_S^*) values, after removing the background noise, which are the sum of the second, third and fourth terms in Eq. (3). Consequently, the PMSE backscatter cross-sections for these radars were calculated. The backscatter cross-section (η), which can be considered as the total isotropically scattered power with an intensity equal to that of the observed backscattered radiation, per unit solid angle, per unit

incident power density and per unit volume of scatterer, is given by

$$\eta = \frac{P_R 4\pi h^4}{P_T e^T e^R \Delta R} \cdot \frac{1}{\int_{\theta=0}^{\pi/2}\int_{\phi=0}^{2\pi} G_T(\theta,\phi) A_R(\theta,\phi) h^2 \sin(\theta)\, d\theta\, d\phi} \quad (4)$$

where P_T is the transmitted peak power, e^T is the system efficiency in transmission, e^R is the system efficiency in reception (as indicated in the calibration equations), h is the echo backscatter height, ΔR is the vertical range resolution, $G_T(\theta,\phi)$ is the antenna gain in transmission, and $A_R(\theta,\phi)$ is the antenna effective area in reception. However, for narrower and moderate beam width radars, the above equation can be safely approximated as follows (see Hocking, 1985):

$$\eta = \frac{32\pi(2\ln 2)h^2 P_R}{G_{TM} A_{RM} (\theta^1_{1/2})^2 e^T e^R P_T (\Delta R \cdot 2)} \quad (5)$$

where G_{TM} is the transmitter antenna gain in the vertical direction, A_{RM} is the effective area of the receiver array in vertical direction and $(\theta^1_{1/2})$ is the HPHW of receiver beam. Care was taken in the estimation of antenna gain as well as system efficiency in determining transmission strengths for all radars used in this study. The antenna gain was carefully calculated using a simulation model, which replicated the exact antenna array structure of each radar system (Swarnalingam, 2007; Swarnalingam et al., 2009). The upper portion of Table 1 shows system specifications and the experimental details of the five radars that have been used in our study.

4.1. Comparing SKiYMET radar results

For the SKiYMET radars, a 512 point coherent integration was applied, giving an effective sampling rate of 0.48 s. Following this, a 42 point incoherent averaging procedure was used. Since Eq. (5) assumes not only volume filling but also isotropically scattered power, special care was taken in the backscatter cross-section estimations, especially with the SKiYMET radars. With regard to the SKiYMET radar, we take advantage of the fact that PMSE echoes originating in the height range 80–90 km will appear in the off-vertical beams at range 92–104 km, and hence will not be confused with the main beam echoes. Furthermore, spectra recorded with the off-vertical beam show Doppler shifts due to horizontal wind motion, and will be suppressed by our large amount of coherent integration. These facts are important to recognize for radar calibration and PMSE backscatter cross-section estimation. While the sky noise is recorded in all nine beams, PMSE echoes at ranges 80–90 km are only significant in the vertical beam.

Fig. 2 shows examples of same day PMSE observations conducted at Yellowknife, Andenes and Resolute Bay. The figure shows the calculated backscatter cross-sections for the data collected on 15 July 2005 at these three locations, plotted in logarithmic scale. The first two panels show the PMSE structure observed by two SKiYMET radars located at Yellowknife (11:30–12:15 UT first panel) and Andenes (07:00–07:50 UT second panel). The third and fourth panels show the PMSE structures observed by the ALWIN radar (06:00–08:00 UT) and Resolute Bay Quartet-Mode radar (00:00–04:00 UT) on the same day. Note that two SKiYEMT radars are nearly identical in configuration (see Table 1). As we will see shortly (in Fig. 4), we also calculated the backscatter cross-section distributions for these two radars for the data collected during our experiment period. We found that the mean backscatter cross-section values of the two SKiYMET radars at Yellowknife and Andenes were very close. While Yellowknife recorded a median of $1.18 \times 10^{-13}\,\mathrm{m}^{-1}$ and geometric mean of $1.38 \times 10^{-13}\,\mathrm{m}^{-1}$, the SkiYMET at Andenes

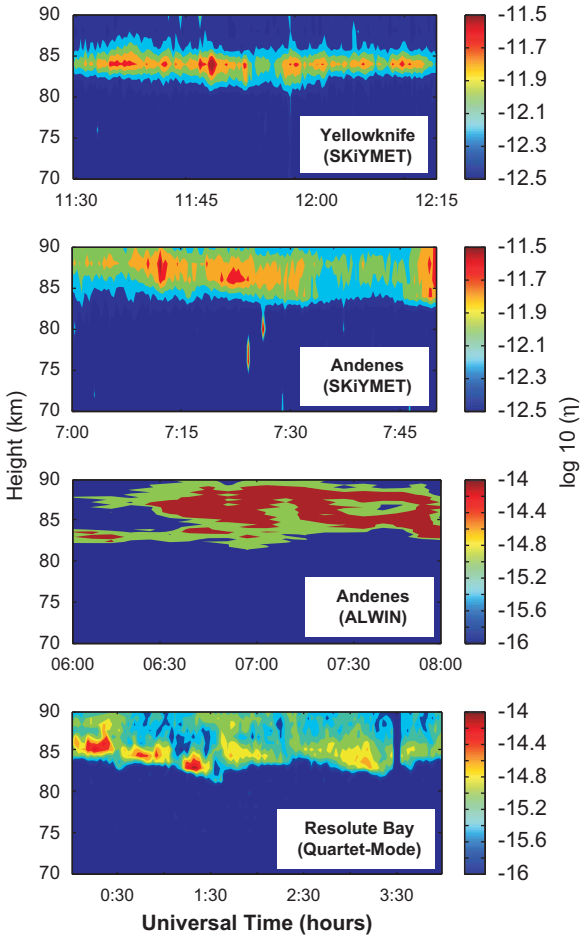

Fig. 2. Same day PMSE experiments conducted at three locations: the upper panel shows height-time contour plot of observed PMSE layers on 15 July 2005 by the SKiYMET radar at Yellowknife. The second panel shows the observed PMSE layers by the SKiYMET radar at Andenes on the same day albeit for difference times. The third and fourth panels also show the same day observations by the Andenes ALWIN radar and Resolute Bay Quartet-Mode radar, respectively.

recorded a median of $1.71 \times 10^{-13}\,\mathrm{m}^{-1}$ and geometric mean of $2.09 \times 10^{-13}\,\mathrm{m}^{-1}$.

4.2. Comparing resolute bay results with ALWIN

The signal processing for the Resolute Bay VHF radar and the Andenes ALWIN radar remain the same as in previous PMSE experiments. In the case of the Resolute Bay radars (both the Main-Mode and Quartet-Mode), 8 bit complementary coded signals were transmitted and then 16 point coherent integration was applied on received echoes. For the ALWIN radar, 16 bit complementary coded signals were transmitted and a 32 point integration was applied. Note that the Resolute Bay (Main-Mode) and ALWIN have similar radar designs. Fig. 3 compares the calculated PMSE backscatter cross-sections at these two radars for the interval 17–19 July 2005. It can be seen in the figure that the PMSE backscatter cross-section values for the Resolute Bay (Main-Mode) radar are significantly lower compared with the backscatter cross-sections calculated for ALWIN.

Eq. (5) for backscatter cross-section is valid for all radars from moderate to narrow beam widths. It may break down with very wide radar beam width, and this may be an issue for the Quartet-Mode, but the errors will be slight. A more important issue here is the possible underestimation of backscatter cross-section due to

Table 1
A summary of the system and experimental parameters (upper part), the calculated backscatter cross-section range values and the equivalent C_N^2 values (lower part) for the five radars used in this study.

	Yellowknife (SKiYMET)	Andenes (SKiYMET)	Resolute Bay (Quartet)	Resolute Bay (Main)	Andenes (ALWIN)
Frequency (MHz)	35.65	32.55	51.5	51.5	53.5
Power (kW)	6	12	12	12	36
ΔR (m)	2000	2000	750	750	300
PRF (Hz)	1072	1072	1200	1200	1250
G_{RM} (dB)	14	14	11.5	24	28
G_{TM} (dB)	6	6	11.5	24	28
e_T (%)	75	66	90	35	80
e_R (%)			59	12	76
HPHW (deg)	5	5	35	2	3
Code	Single	Single	8-bit	8-bit	16-bit
Coherent integration	512-point	512-point	16-point	16-point	32-point
Median of η (m^{-1})	1.18E−13	1.71E−13	2.74E−15	3.02E−15	3.51E−14
Geometric mean of η (m^{-1})	1.38E−13	2.09E−13	3.71E−15	4.38E−15	3.18E−14
90th Percentile of η (m^{-1})	7.70E−13	7.41E−13	2.03E−14	4.23E−14	1.64E−12
10th Percentile of η (m^{-1})	3.53E−14	6.54E−14	1.25E−15	9.84E−16	5.63E−16
C_N^2 (using median)	2.51E + 15	1.35E + 15	2.23E + 14	2.47E + 14	3.29E + 15

For SKiYMET e_R is included in G_S^*.

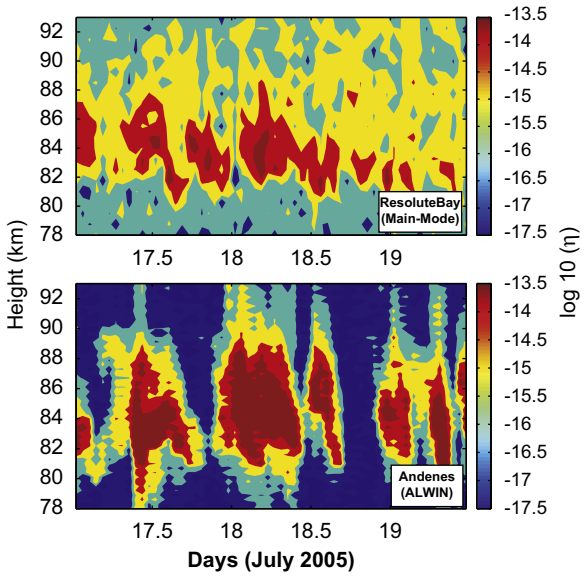

Fig. 3. PMSE observations by two narrow beam MST radars: figure compares the PMSE structures observed by the Resolute Bay radar (Main-Mode) and ALWIN radar during 17–19 July 2005. The upper panel shows height-time contour plot for backscatter cross-sections at Resolute Bay, while the lower panel shows the observed PMSE structure at Andenes during the same interval.

the aspect sensitivity of PMSE scatterers. If the scatterers are anisotropic, the degree of anisotropy will impact the relation between the received power and the back-scatter cross-section. In order to examine this, we have carried out aspect-sensitivity study for a decade long data collected by the Main-Mode radar during 1998–2008 (Swarnalingam and Hocking, 2009). We found that the echoes are aspect sensitive. While a strong aspect nature of scatterers with mean aspect angle, $\theta_s \sim 9^\circ$ (e^{-1} half-width) appears at around 83–85 km, more isotropic scatterers appear at higher altitudes. Similar studies were also conducted at the Poker Flat radar using four years data by Huaman and Balsley (1998), and they also noticed the same features in PMSE. Furthermore, our estimated θ_s values show good agreement with the Poker Flat values. As discussed by Swarnalingam et al. (2009), the calculated aspect angle does not affect the backscatter measurements to any significant level for vertically pointing narrow beam radars such as Resolute Bay Main-Mode and ALWIN. But it will indeed affect the measurements from the wider beam Quartet-Mode radar. Following this, we estimated the effective beam width for the Quartet-Mode radar using the method described by Hocking (1987),

$$\sin^{-2}(\theta^{\mathrm{T}}_{\mathrm{eff}1/2}) = \sin^{-2}(\theta^{\mathrm{T}}_{1/2}) + \sin^{-2}(\theta_{s1/2}) \quad (6)$$

where $\theta_{s1/2}$ is HPHW of the backscatter polar diagram of the scatterers, $\theta^{\mathrm{T}}_{1/2}$ is two-way HPHW of radar and $\theta^{\mathrm{T}}_{\mathrm{eff}\,1/2}$ is the resultant effective HPHW of the combined two-way polar diagram. From our calculations, it was found that the Quartet-Mode radar has a one-way effective beam width $\theta^{1}_{\mathrm{eff}\,1/2} = 10^\circ$. The backscatter cross-sections for the Quartet-Mode were then estimated using the effective beam width, and it was found that the values are comparable with the values of Main-Mode radar. A contour plot for the estimated backscatter cross-sections on 15 July 2005 in the Quartet-Mode radar (00:00–03:45 UT) is shown in the bottom panel of Fig. 2. As discussed in Section 4.1, the figure also shows the same day PMSE observations (15 July 2005) from the two SKiYMET radars (the first two panels) and ALWIN radar (third panel).

Finally, Fig. 4 shows the logarithmic histograms of the calculated backscatter cross-sections for the five radars. In this study, for each radar, all experimental days were included regardless of whether PMSE appeared or not on that radar. For each pre-determined time bin (2 min), the maximum radar returns from the height range 80–90 km were considered, and the distributions of backscatter cross-section were calculated for all five radars after careful noise substraction. It can be seen from the figure that the calculated backscatter cross-section distributions for the Resolute Bay Main-Mode radar and Quartet-Mode radar are comparable. While the Main-Mode recorded a median of $3.02 \times 10^{-15}\,\mathrm{m}^{-1}$ the Quartet-Mode recorded $2.74 \times 10^{-15}\,\mathrm{m}^{-1}$. On the other hand, the ALWIN radar recorded a median of $3.51 \times 10^{-14}\,\mathrm{m}^{-1}$.

5. Discussions

While Fig. 4 compares the calculated backscatter cross-section distributions for all five radars, the lower portion of Table 1 summarizes the median, geometric mean, 10th and 90th percentile values of the distributions. The SKiYMET radars at Yellowknife and Andenes recorded almost the same range of backscatter

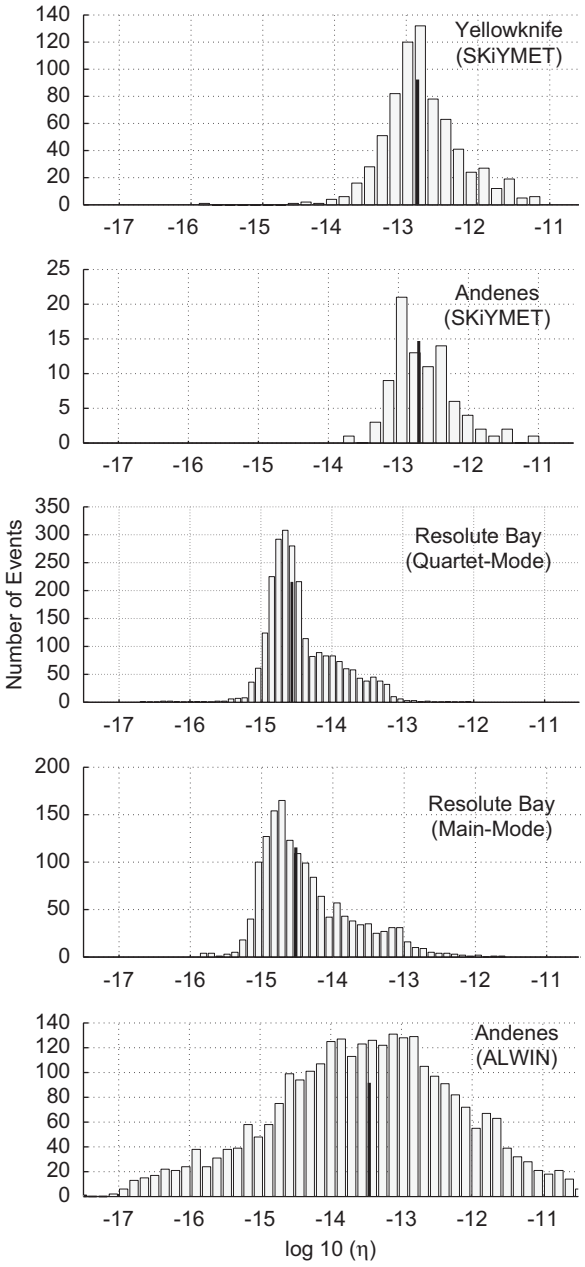

Fig. 4. Comparison of estimated backscatter cross-section distributions of the five radars that has been used in our study. The dark lines refer to the median of the distribution.

cross-section values. But the recorded backscatter cross-section values using the Main-Mode and Quartet-Mode radars at Resolute Bay are about an order of magnitude lower than the ALWIN backscatter cross-section range, and about two orders of magnitude lower than the SKiYMET backscatter cross-section at Yellowknife and Andenes. Note that the Resolute Bay (Main-Mode) and Andenes ALWIN have similar radar design, and the PMSE experiments were conducted simultaneously at these locations for the month of July 2005.

The three MST radars are operated at a frequency in the order of 50 MHz, whereas the two SKiYMET radars are operated in the order of 30 MHz. Since the radar backscatter depends on frequency, we cannot use the estimated backscatter cross-sections for inter-comparison purposes, especially MST radars with SKiYMET. We therefore used a better independent quantity, which is the electron density structure function constant. The electron density structure function constant, which is denoted by C_N^2, is a measure of degree of electron density fluctuation and thus an ideal parameter to compare our results

$$C_N^2 = \frac{C_n^2}{\left(\frac{\partial n}{\partial N}\right)^2} \tag{7}$$

where C_n^2 is the refractive index structure constant, and equal to $(\eta/0.38)\lambda^{1/3}$. The quantity $(\partial n/\partial N)$ is equal to $-r_e\lambda^2/(2\pi)$ at VHF, where r_e is the classical electron radius (see Hocking and Vincent, 1982).

PMSE backscatter cross-section values for the five radars were converted into the equivalent C_N^2 values. It was found that C_N^2 for Resolute Bay is a factor of 10 lower than that for Yellowknife and Andenes (see Table 1). Note that if the radar volume filling condition was not satisfied during the experiments, Eq. (4) would lead to an underestimation in our backscatter cross-section values, and hence under estimation of C_N^2 values. Since the SKiYMET radars have a larger radar volume compared with the Resolute Bay Main-Mode radar and the ALWIN radar by a factor of 17, such scenarios will have greatest impact on SKiYMET radar estimations. Therefore, we can safely say that the strength of PMSE at Resolute Bay is significantly lower compared with strengths at Yellowknife and Andenes.

The Resolute Bay site is located close to both the magnetic north pole (82.7°N, 114.4°W) and geomagnetic north pole (79.7°N, 71.8°W), and this may play an important role in determining the strength of the PMSE. We recall here an important point discussed by Morris et al. (2005), that PMSE are influenced by electron precipitation, which is more prevalent in the auroral oval. Furthermore, the dependence of PMSE on the background electron number density was investigated by Rapp et al. (2002), and they estimated that a minimum of 300–500 electrons per cm^3 are necessary for PMSE to exist. The relationship between PMSE and electron precipitation has not yet been investigated in detail at various locations. Precipitation could play an important role, especially in determining PMSE strengths as a function of latitude and longitude. The formation of electron density gradients by electron precipitation may perhaps be more important than the general electron density increase itself.

We also investigated the level of geomagnetic activity by comparing K_p index values from College (64°N, 147°W) and Tromsø (70°N, 19°E), which are close to Yellowknife and Andenes respectively, and also from Longyearbyen (78.2°N, 15.8°E). During our PMSE experimental days, the K_p index reached a value 6 or higher on many occasions at College and Tromsø (9 days), and also at Longyearbyen (5 days). Note that while the radar sites at Yellowknife, Andenes and Longyearbyen are sometimes located under the auroral oval (depending on diurnal time and level of magnetic activity), the Resolute Bay radar remains a true polar cap site for both the lowest and highest K_p index values (see Morris et al., 2005). These results are also consistent with the fact that PMSE have high occurrence rates at Longyearbyen (geomagnetic latitude 75°N) compared with at Resolute Bay (see Lübken et al., 2004).

6. Conclusions

New studies of PMSE with five radars (two SKiYMET radars, two MST narrow beam radars and a MST wider beam radar) at three northern hemisphere locations have been presented. The two SKiYMET radars (located at Yellowknife and Andenes) are near identical radars. The two MST narrow beam radars (located at Resolute Bay and Andenes) have similar design. By

applying the same method of noise calibration and signal processing, the calibrated PMSE signal strengths at these sites were compared using the data collected during the boreal summer of 2005. Comparison of the two SKiYMET radar backscatter cross-sections shows that the PMSE strengths at Yellowknife and Andenes are similar. Comparison of two MST radar backscatter cross-sections shows that PMSE strength at Resolute Bay is significantly lower than Andenes. Furthermore, we compared the electron density fluctuations at these three locations using the electron density structure function constant (C_N^2). While electron density fluctuations at Yellowknife and Andenes look to be similar, the fluctuations at Resolute Bay are significantly weaker. This could be due to the fact that the radar site is located closer to the magnetic and geomagnetic north poles and is never located under the auroral oval, even for high or low K_p levels. Our results also show that SKiYMET (and similar) radars can be useful for PMSE studies, and this will allow more extensive network of such radars to be utilized further for this purpose in the future.

Acknowledgment

The authors thank Dr. Tom Landecker, Dominion Radio Astrophysical Observatory in Penticton, Canada for providing sky survey data. Authors also acknowledge to Tromsø Geophysical Observatory, (University of Tromsø, Norway and Space Weather Prediction Center (NOAA), Boulder, Colorado, USA) for providing geomagnetic data.

References

Bridle, A.H., 1967. The spectrum of the radio background between 13 and 404 MHz. Mon. Not. R. Astr. Soc. 136, 219–240.

Campistron, B., Despaux, G., Lothon, M., Klaus, V., Mauprivez, M., 2002. A partial 45 MHz sky temperature map obtained from the observations of five ST radars. Ann. Geophys. 19, 863–871.

Cane, H.V., 1978. A 30 MHz map of the whole sky. Aust. J. Phys. 31, 561–565.

Cho, J.Y.N., Kelley, M.C., 1993. Polar mesosphere summer radar echoes: observations and current theories. Rev. Geophys. 31 (3/August), 243–265.

Czechowsky, P., Rüster, R., 1985. Power spectra of mesospheric velocities in polar regions. Handbook of MAP 18, 207–211.

Ecklund, W.L., Balsley, B.B., 1981. Long-term observations of the Arctic mesosphere with the MST radar at Poker Flat, Alaska. J. Geophys. Res. 86 (A9), 7775–7780.

Garcia, R.R., Solomon, S., 1985. The effect of breaking gravity waves on the dynamics and chemical composition of the mesosphere and lower thermosphere. J. Geophys. Res. 90 (D2), 3850–3868.

Haslam, C.G.T., Klein, U., Salter, C.J., Stoffel, H., Wilson, W.E., Cleary, M.N., Cooke, D.J., Thomasson, P., 1981. A 408 MHz all-sky continuum survey. Astron. Astrophys. 100, 209–219.

Hocking, W.K., 1985. Measurement of turbulent energy dissipation rates in the middle atmosphere by radar techniques: a review. Radio Sci. 20 (6), 1403–1422.

Hocking, W.K., 1987. Radar studies of small scale structure in the upper middle atmosphere and lower ionosphere. Adv. Space. Res. 7 (10), 327–338.

Hocking, W.K., Röttger, J., 1997. Studies of polar mesosphere summer echoes over EISCAT using calibrated signal strengths and statistical parameters. Radio Sci. 32 (4), 1425–1444.

Hocking, W.K., Vincent, R.A., 1982. Comparative observations of D region HF partial reflections at 2 and 6 MHz. J. Geophys. Res. 87, 7615–7624.

Hoppe, U.P., Hall, C., Röttger, J., 1988. First observation of summer polar mesosphere backscatter with a 224 MHz radar. Geophys. Res. Lett. 15 (1), 28–31.

Huaman, M.M., Balsley, B.B., 1998. Long-term-mean aspect sensitivity of PMSE determined from poker flat MST radar data. Geophys. Res. Lett. 25, 947–950.

Huaman, M.M., Kelley, M.C., Hocking, W.K., Woodman, R.F., 2001. Polar mesosphere summer echo studies at 51.5 MHz at Resolute Bay, Canada: comparison with Poker Flat results. Radio Sci. 36, 1823–1837.

Inhester, B., Ulwick, J.C., Cho, J.Y.N., Kelley, M.C., Schmidt, G., 1990. Consistency of rocket and radar electron density observations: implication about the anisotropy of mesospheric turbulence. J. Atmos. Terr. Phys. 52 (10/11), 855–873.

Jarvis, M.J., Clilverd, M.A., Rose, M.C., Rodwell, S., 2005. Polar mesosphere summer echoes (PMSE) at Halley (76S, 27W), Antarctica. Geophys. Res. Lett. 32.

Kelley, M.C., Ulwick, J.C., 1988. Large- and small-scale organization of electrons in the high-latitude mesosphere: implications of STATE data. J. Geophys. Res. 93, 7001–7008.

Kirkwood, S., Wolf, I., Nilsson, H., Dalin, P., Mikhaylova, D., Belova, E., 2007. Polar mesosphere summer echoes at Wasa, Antarctica (73°S): first observations and comparison with 68°N. Geophys. Res. Lett. 34, 9–10.

Landecker, T.L., Wielebinski, R., 1970. The galactic metre wave radiation: a two-frequency survey between declinations $+25^\circ$ and -25° and the preparation of a map of the whole sky. Aust. J. Phys. Suppl. 16, 1–30.

Lübken, F.J., Zecha, M., Höffner, J., Röttger, J., 2004. Temperatures polar mesosphere summer echoes, and noctilucent clouds over Spitsbergen (78°N). J. Geophys. Res. 109 (D), 11203–11217.

Morris, R.J., Murphy, D.J., Klekociuk, A.R., Holdsworth, D.A., 2007. First complete season of PMSE observations above Davis, Antarctica, and their relation to winds and temperatures. Geophys. Res. Lett. 34, doi:10.1029/2006GL028641.

Morris, R.J., Terkildsen, M.B., Holdsworth, D.A., Hyde, M.R., 2005. Is there a casual relationship between cosmic noise absorption and PMSE?. Geophys. Res. Lett. 32 (24) doi:10.1029/2005GL024568.

Rapp, M., Gumbel, J., Lübken, F.J., Latteck, R., 2002. D region electron number density limits for the existence of polar mesosphere summer echoes. J. Geophys. Res. 107 (19) doi:10.1029/2001JD001323.

Rapp, M., Lübken, F.J., 2004. Polar mesosphere summer echoes (PMSE): review of observations and current understanding. Atmos. Chem. Phys. 4, 2601–2633.

Roger, H.V., Costain, C.H., Landecker, T.L., Swerdlyk, C.M., 1999. The radio emission from the Galaxy at 22 MHz. Astron. Astrophys. Suppl. Ser. 137, 7–11.

Röttger, J., 2001. Observations of the polar D-region and the mesosphere with the EISCAT Svalbard Radar and SOUSY Svalbard Radar. Mem. Nat. Inst. Pol. Res. 54, 9–20.

Röttger, J., La Hoz, C., 1990. Characteristics of polar mesosphere summer echoes (PMSE) observed with the EISCAT 224 MHz radar and possible explanations of their origin. J. Atmos. Terr. Phys. 52 (10/11), 893–906.

Röttger, J., La Hoz, C., Kelley, M.C., Hoppe, U.P., Hall, C., 1988. The structure and dynamics of polar mesosphere summer echoes observed with the EISCAT 224 MHz radar. Geophys. Res. Lett. 15 (12), 1353–1356.

Schmidt, G., Ruster, R., Czechowsky, P., 1979. Complementary code and digital filtering for detection of weak VHF radar signals from the mesosphere. IEEE Trans. Geosci. Electron. GE-17 (4), 154–161.

Sironi, G., 1974. The spectrum of the galactic non-thermal background radiation—I. Mon. Not. R. Astr. Soc. 166, 345–353.

Swarnalingam, N., 2007. Studies of polar mesosphere summer echoes at multiple sites using calibrated radars. Ph.D. Thesis, University of Western Ontario, Canada.

Swarnalingam, N., Hocking, W.K., 2006. Calibration and calculation of absolute backscatter cross-section using sky noise and calibrated noise source for Resolute Bay radar. The 11th Workshop on Technical and Scientific Aspects of MST Radar—December 2006, Tirupati, India.

Swarnalingam, N., Hocking, W.K., 2007. Calibration and calculation of absolute backscatter cross-section using sky noise and calibrated noise source for Resolute Bay radar. In: Anandan, V.K. (Ed.), Proceedings of the 11th Workshop on Technical and Scientific Aspects of MST Radar—December 2006, pp. 328–333.

Swarnalingam, N., Hocking, W.K., 2009. A decade-long aspect-sensitivity studies of polar mesosphere summer echoes at Resolute Bay. The 12th Workshop on Technical and Scientific Aspects of MST Radar—May 2009, London, Canada.

Swarnalingam, N., Hocking, W.K., Argall, P.S., 2009. Radar efficiency and the calculation of decade-long PMSE backscatter cross-section for Resolute Bay VHF radar. Ann. Geophys. 27 (4), 1643–1656.

Turtle, A.J., Baldwin, J.E., 1962. A survey of galactic radiation at 178 Mc/s. Mon. Not. R. Astr. Soc. 124 (6), 459–476.

Webster, A.S., 1974. The spectrum of the galactic non-thermal background radiation—II. Mon. Not. R. Astr. Soc. 166, 355–371.

Woodman, R.F., 2003. Coordinated hemispheric and interhemispheric observations of polar mesosphere summer echoes (PMSE). In: Chau, J., Lau, J., Röttger, J. (Eds.), Proceedings of the 10th Workshop on Technical and Scientific Aspects of MST Radar, p. 36.

Woodman, R.F., Balsley, B.B., Aqunio, F., Flores, L., Vazques, E., Sarango, M., Huaman, M.M., Soldi, H., 1999. First observation of polar mesosphere summer echoes in Antarctica. J. Geophys. Res. 104 (A10), 22577–22590.